Sains Malaysiana 55(10)(2026): 1664-1680
http://doi.org/10.17576/jsm-2026-5510-06

Untargeted Muscle Tissue Metabolites Profiling in an Ageing Animal Model Supplemented with Ginger Active Compounds

(Profil Metabolit Tisu Otot Tidak Bersasar dalam Model Haiwan Penuaan yang Disuplementasi dengan Sebatian Aktif Halia)

NUR FATIN NABILAH MOHD SAHARDI[1], NUR FATHIAH ABDUL SANI[2], JEN KIT TAN[2,4], MARIAM FIRDHAUS MAD NORDIN[3] & SUZANA MAKPOL[2,4,*]

[1]*Secretariat Research and Innovation, Faculty of Medicine, Universiti Kebangsaan Malaysia, Jalan Yaacob Latif, Bandar Tun Razak, Cheras, 56000 Kuala Lumpur, Malaysia*
[2]*Department of Biochemistry, Faculty of Medicine, Level 17 Preclinical Building, Universiti Kebangsaan Malaysia, Jalan Yaacob Latif, Bandar Tun Razak, Cheras, 56000 Kuala Lumpur, Malaysia*
[3]*AM Zaideen Ventures Sdn Bhd, Kuala Lumpur, Malaysia*
[4]*Ageing and Degenerative Diseases Research Group, Universiti Kebangsaan Malaysia, 43600 UKM Bangi, Selangor, Malaysia*

Received: 22 April 2026/Accepted: 23 September 2026

*Corresponding author; email: suzanamakpol@ukm.edu.my

ABSTRACT

Age-related muscle loss is a significant health concern among older adults, contributing to frailty, reduced strength, and functional decline, with oxidative stress identified as a key underlying driver of this deterioration. Ginger (*Zingiber officinale* Roscoe), a traditional herb with established antioxidant properties, has shown potential to mitigate oxidative damage. However, its effects on muscle metabolic regulation during the ageing process remain largely unexplored. Therefore, this study aimed to investigate the effects of ginger extract on metabolic pathways associated with age-related muscle loss. Sprague-Dawley rats of various ages (young, adult, and old) were administered distilled water or ginger extract (200 mg/kg body weight) daily for three months. Muscle tissues were subjected to untargeted metabolomic profiling using UHPLC-MS/MS. Correlation analyses were conducted to determine associations between significantly altered metabolites and oxidative stress and inflammatory markers. Untargeted metabolomic profiling showed that ageing markedly altered muscle metabolites, particularly those in the phenylalanine, tyrosine, and tryptophan biosynthesis pathway. Ginger supplementation partially reversed these age-associated shifts; most notably, it significantly downregulated β-muricholic acid and xanthosine in old rats, which had increased during ageing. Furthermore, ginger treatment upregulated γ-L-glutamyl-L-glutamic acid, suggesting enhanced antioxidant capacity and muscle regenerative pathways. These findings suggest that ginger extract may attenuate age-related physiological decline by modulating several key metabolites disrupted during ageing, highlighting its potential as a supplement to support healthy ageing in older individuals.

Keywords: Ginger extract; metabolomic study; muscle ageing; oxidative stress

ABSTRAK

Kehilangan otot berkaitan usia merupakan isu kesihatan yang signifikan dalam kalangan warga emas yang menyumbang kepada kerapuhan, penurunan kekuatan dan kemerosotan fungsi, dengan tekanan oksidatif dikenal pasti sebagai pemacu utama kepada kemerosotan otot. Halia (*Zingiber officinale* Roscoe), sejenis herba tradisional yang mempunyai sifat antioksidan yang terbukti, telah menunjukkan potensi dalam mengurangkan kerosakan oksidatif. Walau bagaimanapun, kesannya terhadap regulasi metabolik otot semasa proses penuaan masih belum banyak dikaji. Oleh itu, penyelidikan ini bertujuan untuk mengkaji kesan ekstrak halia terhadap laluan metabolik yang berkaitan dengan kehilangan otot akibat penuaan. Tikus Sprague-Dawley daripada pelbagai peringkat umur (muda, dewasa dan tua) diberikan air suling atau ekstrak halia (200 mg/kg berat badan) setiap hari selama tiga bulan. Tisu otot dianalisis menggunakan pemprofilan metabolit tidak bersasar dengan UHPLC-MS/MS. Analisis korelasi dijalankan untuk menentukan hubungan antara metabolit yang berubah secara signifikan dengan penanda tekanan oksidatif dan keradangan. Hasil pemprofilan metabolomik tidak bersasar menunjukkan bahawa penuaan secara ketara mengubah metabolit otot, khususnya dalam laluan biosintesis fenilalanina, tirosin dan triptofan. Suplementasi halia didapati sebahagiannya membalikkan perubahan berkaitan usia ini; yang paling ketara,

ia menurunkan secara signifikan asid β-murikolik dan xantosin dalam tikus tua, yang meningkat semasa proses penuaan. Selain itu, rawatan halia meningkatkan asid γ-L-glutamil-L-glutamik, yang mencadangkan peningkatan kapasiti antioksidan dan laluan regenerasi otot. Keputusan ini menunjukkan bahawa ekstrak halia berpotensi memperlahankan kemerosotan fisiologi berkaitan usia dengan memodulasi beberapa metabolit utama yang terganggu semasa proses penuaan, sekali gus menonjolkan potensinya sebagai suplemen untuk menyokong penuaan sihat dalam kalangan individu berusia.

Kata kunci: Ekstrak halia; kajian metabolik; penuaan otot; tekanan oksidatif

INTRODUCTION

Age-related muscle dysfunction or sarcopenia is a common problem affecting older people aged 60 years and above (Dao et al. 2020). Sarcopenia is the loss of skeletal muscle strength and function (Cruz-Jentoft et al. 2019). It is characterised by decreased skeletal muscle mass, strength, and function, which increases the risk of disability, fall-related injuries, and frailty among the elderly (Cruz-Jentoft et al. 2019). The cause of sarcopenia is multifactorial, involving physiological, genetic and environmental factors (Cruz-Jentoft & Sayer 2019). Sarcopenia is associated with hormonal changes, elevated oxidative stress, and inadequate nutritional intake (Liguori et al. 2018; Yuan & Larsson 2023). However, increased oxidative stress is a major cause of sarcopenia (Liguori et al. 2018).

Oxidative stress is a primary driver of sarcopenia, arising from an imbalance between the production of reactive oxygen species (ROS), particularly hydroxyl radical (·OH), hydrogen peroxide (H_2O_2), superoxide anion ($O_2\cdot^-$), and nitric oxide (NO), and the body's antioxidant defence (Sahoo et al. 2022; Sies, Berndt & Jones 2017). The excessive production of these ROS leads to significant oxidative damage to proteins and lipids, triggering an inflammatory response that disrupts cellular homeostasis (Sahoo et al. 2022). Crucially, this oxidative environment shifts the metabolic equilibrium of muscle tissue by impairing protein synthesis pathways, including mTOR signalling. At the same time, it accelerates protein degradation through increased autophagy and apoptosis. This persistent imbalance between synthesis and degradation ultimately contributes to progressive loss of skeletal muscle mass and function characteristic of age-related muscle wasting (Cannataro et al. 2021).

Additionally, muscle loss is associated with changes in the muscle tissue metabolome. A previous study found that changes in specific metabolites, including glucose, phospholipids, and polyamines, occurred in the aged skeletal muscle mass of mice (Uchitomi et al. 2019). They reported that glucose metabolism products, such as dihydroxyacetone phosphate and fructose 1,6-diphosphate, decreased due to a reduction in glycolytic muscle fibres. Meanwhile, changes in phospholipid metabolism may reflect alterations in cell membrane phospholipids in aged skeletal muscle. Uchitomi et al. (2019) also found that the levels of acetylcholine, histamine, and serotonin in old skeletal muscle mice were increased. The rise in acetylcholine levels could potentially counteract the decline in neuromuscular junctions that occur with age. At the same time, the elevations in histamine and serotonin might be linked to muscle damage associated with ageing.

Recent research has explored various antioxidant compounds for their potential to mitigate age-related muscle decline. For instance, supplementation with nicotinamide riboside has been shown to enhance the NAD^+ metabolome and induce anti-inflammatory signatures in human skeletal muscle (Elhassan et al. 2019). Similarly, treatment with a tocotrienol-rich fraction (TRF) in aged rats has been shown to improve energy metabolism and stimulate muscle regeneration by upregulating amino acid levels, including phenylalanine and tryptophan (Saud Gany et al. 2022).

Despite these promising findings, the influence of ginger (*Zingiber officinale* Roscoe), a herb recognised for its potent antioxidant and anti-inflammatory activities (Mohd Sahardi & Makpol 2019), on skeletal muscle metabolism during ageing remains insufficiently understood. Therefore, this study aimed to investigate the effects of ginger extract on the muscle metabolome of aged rats, with particular emphasis on its role in modulating age-associated metabolic alterations.

MATERIALS AND METHODS

GINGER (*Zingiber officinale* Roscoe) PREPARATION

Fresh ginger was obtained from Bentong, Pahang, Malaysia. The extraction process was performed at the Department of Chemical Process Engineering, Universiti Teknologi Malaysia (UTM, Kuala Lumpur, Malaysia) and ERP Two One Technologies & Innovations Sdn Bhd (Subang, Malaysia). The voucher specimens were identified and deposited at the Herbarium of Universiti Kebangsaan Malaysia (UKM), Bangi (ID016/2021). The ginger was extracted using subcritical water extraction at an optimum temperature of 130 °C for 30 min with a solvent-to-solid ratio at 28/2 mL/mg (Sarip 2012). This standardised extraction process yielded high concentrations of key bioactive compounds, specifically 289.531 ug/mL of 6-gingerol and 15.466 ug/mL of 6-shogaol. The extract was then freeze-dried and stored at -20 °C until further use.

ANIMAL MODELS AND ETHICAL COMPLIANCE

The experimental protocol was strictly conducted in accordance with ethical guidelines and received prior approval from the Universiti Kebangsaan Malaysia Animal Ethics Committee (UKMAEC Approval Number: BIOK/PP/2018/SUZANA/14-MAY/924-JUNE-2018-MAY-2020). A total of 60 male Sprague-Dawley (SD) rats were used, comprising 20 young (3-month-old), 20 adult (9-month-old), and 20 aged (21-month-old). Within each group, the animals were allocated to the control (n=10) and ginger-treated groups (n=10), based on the animal numbers reported in a previous study by Abdul Sani et al. (2014). No formal a priori power analysis was performed to determine the sample size. During the experimental period, two rats in the aged control group died, resulting in a final sample size of 8 rats in the aged control group and 10 rats in the aged ginger-treated group. All rats were purchased from Universiti Kebangsaan Malaysia Laboratory Animal Resource Unit (LARU). Prior to the experiment, the rats weighing 200-250 g were selected and acclimatised for 7 days. During the acclimatisation and experimental periods, the rats were housed individually in polycarbonate cages at 24 °C, with a 12-h light-dark cycle. The rats were given a rat pellet (Gold Coin, Malaysia) and water *ad libitum*. The rat pellet consisted of a maximum of 5.0% crude fibre content, a minimum of 22.0% crude protein content, a minimum of 3.0% crude fat content, 0.8%-1.2% calcium, a maximum of 13.0% moisture, a maximum of 8.0% ash, 0.6%-1.0% phosphorus, and approximately 49.0% nitrogen-free extract. Kenaf (Muhaaz Enterprise Terengganu, Malaysia) was used for bedding and changed twice weekly.

Following the 7-day acclimatisation period, rats within each age group were randomly allocated to either a control group (n = 10) or a ginger-treated group (n = 10). The control group received 1 mL of distilled water, while the ginger-treated group received ginger extract at 200 mg/kg body weight by oral gavage once daily for 90 days (Figure 1). Animal health and general welfare were monitored daily throughout the study in accordance with the approved animal ethics protocol. The timeline for this study is displayed in Figure 1. The inflammatory and oxidative stress markers were determined by analysing plasma levels of creatine kinase MM (CK-MM), malondialdehyde (MDA), catalase (CAT), superoxide dismutase (SOD), lipid hydroperoxide (LPO), and urine 15-isoprostane F2t. Other studies have documented findings on markers of inflammation and oxidative stress (Makpol et al. 2020; Razak et al. 2023).

EUTHANASIA OF ANIMALS

In this study, a KTX agent, which consists of ketamine, xylazine, and zoletil-50 (tiletamine and zolazepam), was used for euthanasia purposes. The KTX agent was administered by intraperitoneal injection at the lower

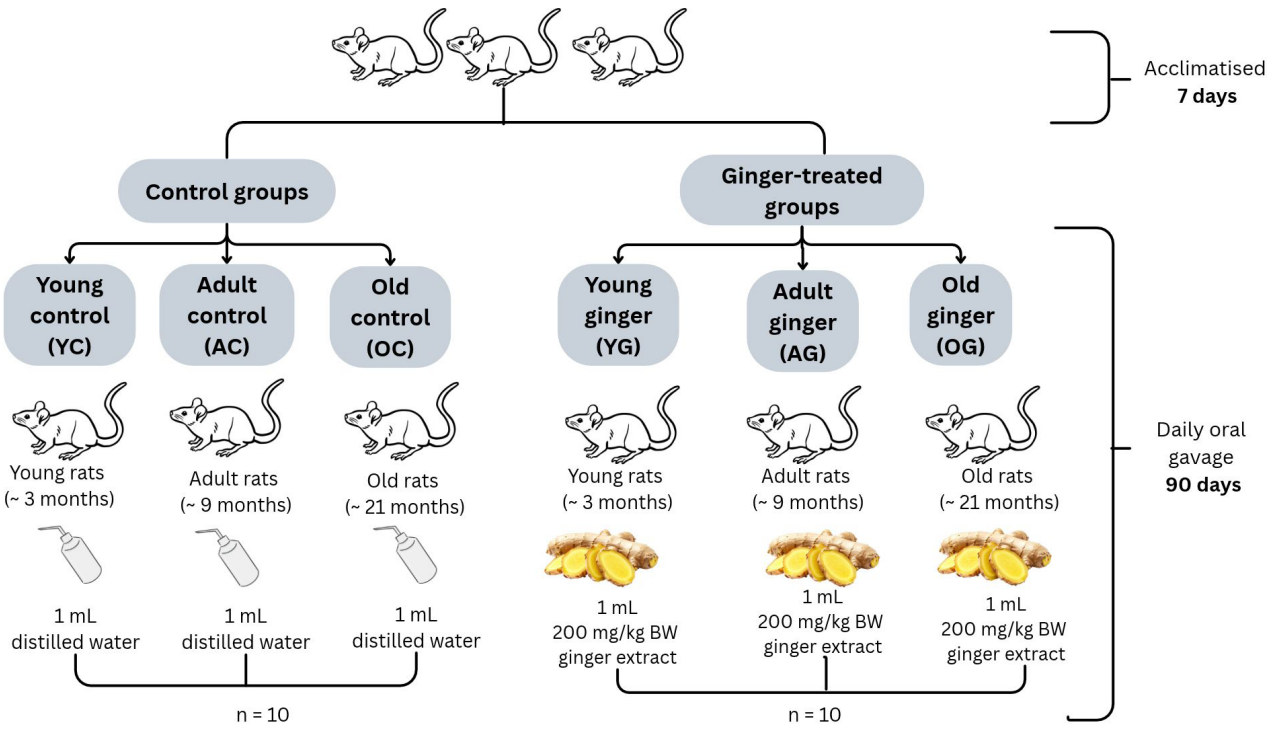


FIGURE 1. Timeline for the experimental protocol

right quadrant of the abdomen at a dose of 0.1 mL/250 g body weight (BW). The rats were then left for 30 min to allow the KTX agent's sedative effect to take effect. The sedative effects were observed through clinical signs, particularly disorientation and loss of consciousness, progressively declining blood pressure and heart rate, rapid, irregular breathing, urination, and defecation. The rats were euthanised by decapitation using a decapitator (Modiezham Sdn. Bhd., Kuala Lumpur, Malaysia).

TISSUE COLLECTION AND SAMPLE PREPARATION

Before necropsy, all rats were fasted overnight for approximately 12 h, with water provided *ad libitum* throughout the fasting period. Following the fasting period, the rats were euthanised, after which necropsy was immediately performed. Following euthanasia, several organs, including the liver, kidneys, and brain, were subsequently dissected and collected. However, for untargeted metabolomic profiling, the gastrocnemius muscle was isolated to characterise metabolic shifts in skeletal muscle tissue. The collected tissue was washed with normal saline (0.9% NaCl), weighed, and stored frozen at -80 °C. For analysis, 1 g of gastrocnemius muscle was cut into smaller pieces with scissors and transferred to a 15 mL tube. 1 mL of mass spectrometry-grade water was added to the sample tube and sonicated with a sonicator (Qsonica, USA) on ice until all samples were homogenised.

METABOLOMIC ANALYSIS BY UHPLC-MS/MS

A total of 100 µL of homogenate was added to a 10 mL glass tube containing 1 µL of Avanti internal standard (Splash Lipidomix) and 800 µL of 100% methanol (MeOH). Then, the tube was vortex-mixed. 1.6 mL 100% Dicromethane (DCM) was added, and the sample was incubated in a vortex at 300 rpm for 1 h at room temperature. After 1 h, 600 µL of distilled water was added to form two layers of the sample. The sample was vortex-mixed. 1.0 mL of the upper phase was collected, dried, and stored at -80 °C. Before performing metabolomic analysis, the sample was reconstituted with 100 µL of 5% MeOH and then filtered using a regenerated membrane syringe filter before being added to the vials. For quality control (QC), 5 µL of all samples were pooled and mixed in a tube, then transferred into a vial (Danial Efendy et al. 2021). Before performing a Liquid Chromatography-Mass Spectrometry analysis, the vials were randomly placed. The sample was analysed using a UHPLC system (Dionex Ultimated 3000, Thermo Scientific) and an Orbitrap-MS (Q Exactive HF, Thermo Scientific). The samples were split into six separate runs. In each of these runs, positive-mode acquisition was completed before transitioning promptly to negative-mode acquisition (Tan et al. 2023). The QC and muscle samples were organised based on a prior study, with minor modifications (Dunn et al. 2011). In summary, the QC sample was introduced at the start, then intermittently after every four samples, and finally at the conclusion of each run. The muscle samples were randomly distributed among the QC injections. Each muscle sample was consecutively injected three times to create technical replicates.

STATISTICAL ANALYSIS

The metabolomic profiles among groups were compared using MetaboAnalyst 5.0. Principal component analysis (PCA) was employed to identify trends within the data and to create visual representations of multidimensional data. ANOVA test, fold change, and pathway analysis were also conducted using MetaboAnalyst software (Xia & Wishart 2016). A false discovery rate (FDR) value < 0.05 was considered a significant metabolite. Pathway analysis of the significant metabolites was also determined using MetaboAnalyst. The pathway was deemed significant and impactful when the p-value < 0.05 and the impact value > 0.1. In addition, Pearson's correlation was used to assess relationships among significant metabolites, oxidative stress, and inflammatory markers, based on results from a previous study (Razak et al. 2023). In Pearson's correlation coefficient classification (r), different ranges of absolute values represent various degrees of correlation: poor correlation (0 to 0.30), moderate correlation (0.30 to 0.50), good correlation (0.50 to 0.70), and strong correlation (0.70 to 1.0) (Guo, Li & Xiao 2020).

RESULTS AND DISCUSSION

Ageing is accompanied by a progressive decline in skeletal muscle function, manifesting as sarcopenia, which significantly compromises mobility and overall quality of life (Cruz-Jentoft & Sayer 2019). This process is associated with pronounced alterations in muscle metabolite profiles, reflecting changes in energy metabolism, oxidative stress, and inflammatory pathways. In the present study, principal component analysis (PCA) demonstrated moderate separation across age groups, with the combined variance explained by PC1 and PC2 ranging from 51.4% to 57.9% in control rats and 42.7% to 57.1% in ginger-treated groups. Specifically, comparisons between young control (YC) and adult control (AC) (PC1: 31.2%; PC2: 20.2%; total: 51.4%), old control (OC) and YC (PC1: 37.2%; PC2: 20.7%; total: 57.9%), and OC and AC (PC1: 45.1%; PC2: 12.8%; total: 57.9%) showed progressive metabolic divergence with age, although overlapping clusters were observed (Figure 2). A similar pattern was observed in the ginger-treated groups, including young ginger (YG) vs. YC (PC1: 36.7%; PC2: 16.6%; total: 53.3%), adult ginger (AG) vs. AC (PC1: 29.8%; PC2: 12.9%; total: 42.7%), and old ginger (OG) vs. OC (PC1: 33.1%; PC2: 21.0%; total: 54.1%), indicating

that ageing induces gradual metabolic remodelling rather than distinct metabolic partitioning. The partial overlap observed between adjacent age groups suggests that metabolic ageing occurs as a continuous process rather than through discrete transitions. This overlap likely reflects a transitional metabolic phenotype, in which adult animals exhibit metabolic characteristics that are intermediate between those of young and old animals. Furthermore, inter-individual biological variability and compensatory metabolic adaptations during ageing may contribute to the shared metabolomic profiles observed among neighbouring age groups (Sebastiani et al. 2024).

To further characterise the metabolic alterations underlying this overall separation, untargeted metabolomics was performed to identify significantly altered metabolites across age groups (Table 1). In AC vs YC, eight metabolites differed significantly, with glycocholic acid and β-muricholic acid showing the highest upregulation (11.363-fold and 6.456-fold, respectively), while hexanoyl carnitine was markedly downregulated (Table 1). The transition from YC to OC showed a more pronounced metabolic shift, with 35 significant metabolites, of which 34 were upregulated. This pattern was largely driven by glycocholic acid and β-muricholic acid, which exhibited substantial increases of 7.695-fold and 4.341-fold, respectively. Similarly, OC vs AC showed 26 significant metabolites were upregulated, including proline, propionyl carnitine, lysine, α-aspartyl phenylalanine, with 2'-deoxycytidine 5'-monophosphate (4.002-fold) showing the highest increase. These findings indicate progressive metabolite accumulation with ageing, reflecting disruptions in lipid metabolism, amino acid turnover, and nucleotide metabolism.

Notably, the consistent elevation of bile acid-related metabolites highlights a potential association between bile acid dysregulation in skeletal muscle metabolism. Among these, bile acids, particularly β-muricholic acid

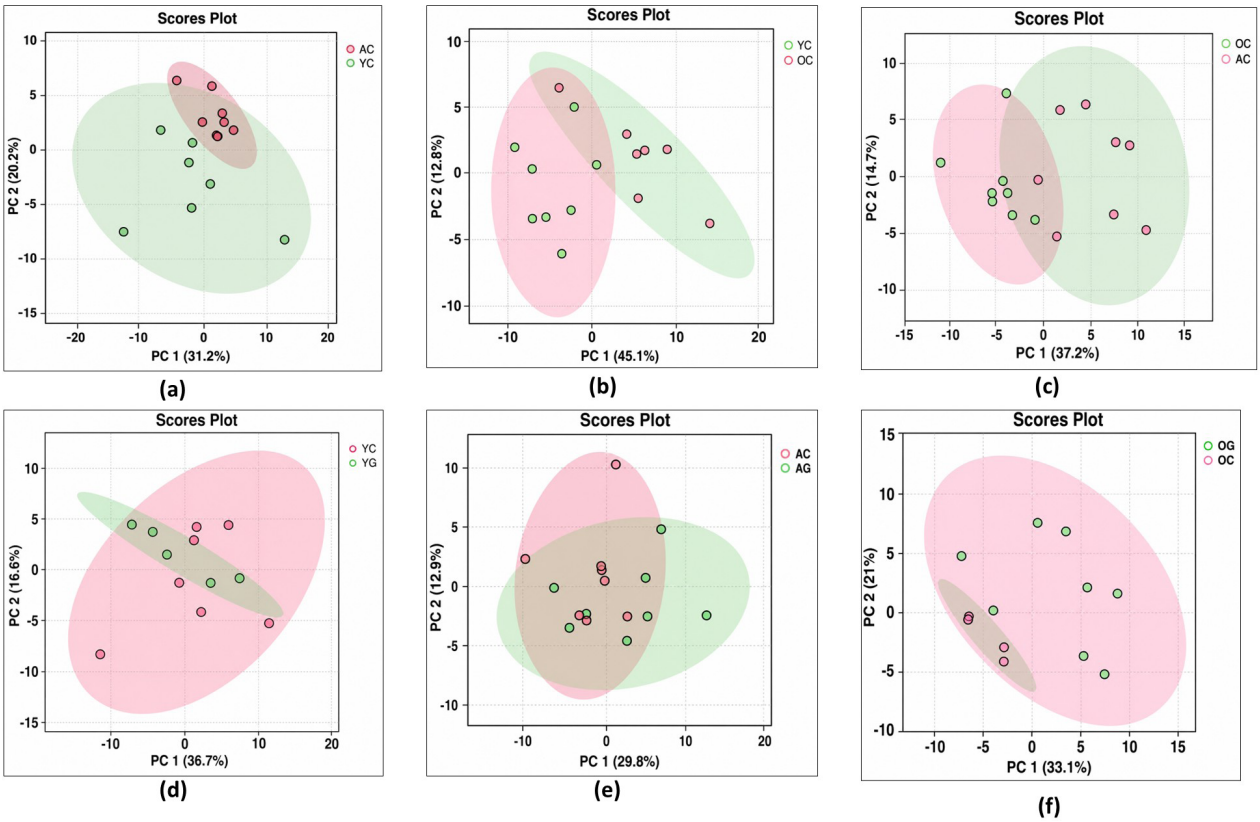


FIGURE 2. PCA score plots for the control and ginger-treated groups. (a) PCA score plot between the young control group (green filled circle) and the adult control group (red filled circle). (b) PCA score plot between the old control group (red filled circle) and young control group (green filled circle), (c) PCA score plot between adult control group (red filled circle) and old control group (green filled circle), (d) PCA score plot between young treatment group (green filled circle) and young control group (red filled circle), (e) PCA score plot between adult treatment group (green filled circle) and adult control group (red filled circle), and (f) PCA score plot between old treatment group (green filled circle) and old control group (red filled circle)

TABLE 1. List of significantly different metabolites among control groups

Mode	Name	MW	RT	ID	FC			Overall P-value	FDR	Significant Tukey HSD comparisons
					AC vs YC	OC vs YC	OC vs AC			
pos	Glycyl-L-leucine	188.116	3.208	HMDB00759	-	+1.997	-	2.72×10^{-5}	3.84×10^{-4}	YC–OC
pos	Trans-3-Indoleacrylic acid	187.06323	3.752	HMDB00734	-	+2.136	+1.718	3.54×10^{-5}	4.38×10^{-4}	YC–OC; AC–OC
pos	N6-Me-Adenosine	281.11198	1.052	MZ 10245	-	+2.269	+1.773	1.05×10^{-4}	9.41×10^{-4}	YC–OC; AC–OC
pos	Proline	115.06344	0.603	HMDB00162/HMDB03411	-	+1.680	+1.724	1.81×10^{-4}	1.38×10^{-3}	YC–OC; AC–OC
pos	Propionyl carnitine	217.13128	2.036	HMDB00824	-	-	+2.104	4.01×10^{-4}	2.09×10^{-3}	AC–OC
pos	Lysine	146.10543	0.421	HMDB00182	-	+1.369	+1.510	5.02×10^{-4}	2.49×10^{-3}	YC–OC; AC–OC
pos	α-Aspartyl phenylalanine	280.10564	3.816	HMDB00706	-	-	+1.785	7.77×10^{-4}	3.19×10^{-3}	AC–OC
pos	2-Hydroxycinnamic acid/4-Coumaric acid	164.04724	1.312	HMDB02641/HMDB02035	-	+1.679	+1.522	8.12×10^{-4}	3.19×10^{-3}	YC–OC; AC–OC
pos	Tryptophan	204.08979	3.751	HMDB00929/HMDB13609	-	+1.712	+1.654	8.17×10^{-4}	3.19×10^{-3}	YC–OC; AC–OC
pos	2,5-Dimethylpyrazine/2,6-Dimethylpyrazine	108.06883	0.484	HMDB35289/HMDB35248	-1.272	-1.255	-	8.38×10^{-4}	3.19×10^{-3}	YC–AC; YC–OC
pos	Coumarin	146.03663	1.314	HMDB01218	-	+1.643	+1.576	1.04×10^{-3}	3.61×10^{-3}	YC–OC; AC–OC
pos	Adenine	135.05421	0.885	HMDB00034	-	+3.589	-	1.06×10^{-3}	3.61×10^{-3}	YC–OC
pos	Leucine/Isoleucine	131.09454	1.504	HMDB00687	-	+1.648	+1.530	1.13×10^{-3}	3.73×10^{-3}	YC–OC; AC–OC
pos	Hexanoyl carnitine	259.17805	5.356	HMDB00705	-2.229	-	+2.931	1.37×10^{-3}	4.36×10^{-3}	YC–AC; AC–OC
pos	Glycylproline	172.08468	0.63	HMDB00721	-	+2.478	+2.405	2.02×10^{-3}	5.89×10^{-3}	YC–OC; AC–OC
pos	Ergothioneine	229.08831	0.652	HMDB03045	-	+2.148	-	2.33×10^{-3}	6.58×10^{-3}	YC–OC
pos	Adenosine 5'-monophosphate/3'-Adenosine monophosphate	347.06259	0.883	HMDB00045/HMDB03540	-	+3.321	-	3.40×10^{-3}	9.09×10^{-3}	YC–OC
pos	Pipecolic acid/Pipecolinic acid	129.07899	0.841	HMDB05960/HMDB00070/HMDB00716	+1.594	+1.651	-	4.29×10^{-3}	1.09×10^{-2}	YC–AC; YC–OC
pos	Creatinine	113.059	0.534	HMDB00562	-	+1.599	-	5.53×10^{-3}	1.30×10^{-2}	YC–OC
pos	Thiamine	264.10413	0.709	HMDB00235	-	+1.820	+1.873	5.79×10^{-3}	1.33×10^{-2}	YC–OC; AC–OC

continue to next page

continue from previous page

pos	Cytidine	243.08531	0.741	HMDB00089	-	+2.423	+2.32	7.59×10^{-3}	1.67×10^{-2}	YC–OC; AC–OC
pos	Hypoxanthine	136.03837	1.099	HMDB00157	-	+1.460	+1.486	8.05×10^{-3}	1.69×10^{-2}	YC–OC; AC–OC
pos	Cytosine/Isocytosine	111.04343	0.741	HMDB00630	-	+2.139	+2.082	8.23×10^{-3}	1.70×10^{-2}	YC–OC; AC–OC
pos	N6, N6, N6-Trimethyl-L-lysine	188.15223	0.513	MZ 909	-	+1.830	-	1.96×10^{-2}	3.23×10^{-2}	YC–OC
neg	Pantothenic acid	219.11009	3.51	HMDB00210	+2.060	-	-	1.20×10^{-6}	2.98×10^{-5}	YC–AC; YC–OC
neg	Malic acid	134.02041	0.681	HMDB00744/ HMDB31518/ HMDB00156	-	+1.604	-	1.34×10^{-5}	2.65×10^{-4}	YC–OC
neg	Glutathione (reduced)	307.08343	0.925	HMDB00125	-	+1.832	+1.588	6.35×10^{-5}	6.29×10^{-4}	YC–OC; AC–OC
neg	Aspartic acid	133.03639	0.492	HMDB00191	-	+1.808	+2.615	1.25×10^{-4}	1.03×10^{-3}	YC–OC; AC–OC
neg	β-Muricholic acid/Cholic acid	408.28746	9.861	HMDB0000415/ HMDB00619	+6.456	+4.341	-	2.43×10^{-4}	1.72×10^{-3}	YC–AC; YC–OC
neg	Phenylalanine	165.07812	3.298	MZ 8	-	+2.386	+2.129	3.10×10^{-4}	1.84×10^{-3}	YC–OC; AC–OC
neg	Arginine	174.11083	0.469	MZ 408	-	+1.522	+1.604	3.19×10^{-4}	1.84×10^{-3}	YC–OC; AC–OC
neg	Tyrosine	181.07303	1.328	HMDB00158	-	+1.479	+1.463	3.35×10^{-4}	1.84×10^{-3}	YC–OC; AC–OC
neg	2’-Deoxycytidine 5’-monophosphate	307.05675	0.784	MZ136	-	+2.272	+4.002	6.24×10^{-4}	2.94×10^{-3}	YC–OC; AC–OC
neg	UDP-N-acetylglucosamine	607.0815	0.634	HMDB00290	-	-	-2.703	7.06×10^{-4}	3.18×10^{-3}	AC–OC
neg	Glycocholic acid	465.30903	8.907	MZ 429	+11.363	+7.695		8.74×10^{-4}	3.21×10^{-3}	YC–AC; YC–OC
neg	Histidine	155.06847	0.475	HMDB00177		+1.659	+1.657	1.59×10^{-3}	4.85×10^{-3}	YC–OC; AC–OC
neg	Adenosine 5’-monophosphate/2’-Deoxyguanosine 5’-monophosphate	347.06271	0.885	HMDB00045/HMDB01044	-	+3.371	-	2.90×10^{-3}	7.96×10^{-3}	YC–OC
neg	β-Leucine	131.09356	2.087	MZ 414	-	+3.082	-	5.18×10^{-3}	1.25×10^{-2}	YC–OC
neg	3-Methylhistidine/1-Methylhistidine/ Methylhistidine	169.08416	0.479	MZ 213/MZ 125/MZ 792	-	-	+1.372	7.87×10^{-3}	1.69×10^{-2}	AC–OC
neg	Xanthosine	284.07543	3.092	HMDB00299	-	+1.861	+2.000	9.12×10^{-3}	1.80×10^{-2}	YC–OC; AC–OC
neg	Taurine	125.01354	0.496	HMDB00251	+1.197	-	-	9.35×10^{-3}	1.81×10^{-2}	YC–AC
neg	4-Oxoproline	129.0415	1.137	MZ 1268	-	+1.675	+1.688	1.12×10^{-2}	2.07×10^{-2}	YC–OC; AC–OC
neg	2-Oxoglutaric acid	146.0205	0.817	HMDB00208	+3.045	-	-	1.20×10^{-2}	2.11×10^{-2}	YC–AC

MW: molecular weight; RT: retention time; FC, fold change; FDR, false discovery rate; YC, young control; AC, adult control; OC, old control. Overall p-values were obtained from one-way ANOVA and adjusted for multiple testing using the false discovery rate method. Metabolites with FDR < 0.05 were considered statistically significant. Significant pairwise differences were identified using Tukey’s HSD post-hoc test. The reported FDR values represent the overall ANOVA FDR and not the FDR for individual Tukey pairwise comparisons. “–” indicates that no significant difference was identified for the respective comparison

and glycocholic acid, were consistently elevated in adult and aged rats, suggesting age-dependent changes in bile acid metabolism. Beyond their classical role in lipid digestion, bile acids also function as signalling molecules that regulate lipid, glucose, and energy metabolism through receptors such as the farnesoid X receptor (FXR) and Takeda G-protein-coupled receptor 5 (TGR5), as well as induction of fibroblast growth factor 15 (FGF15) in mice or its human analogue, FGF19 (Fleishman & Kumar 2024). Previous studies have reported altered expression of FXR and TGR5 in the skeletal muscle of individuals with sarcopenia, suggesting a potential association with pathways involved in muscle protein synthesis and energy metabolism (Jia, Liu & Liu 2025). Likewise, reduced TGR5 signalling in aged muscle has been associated with impaired mitochondrial function and decreased glucose uptake, whereas dysregulation of FXR signalling has been linked to alterations in mTOR signalling and autophagy (Keitel, Stindt & Häussinger 2019). As β-muricholic acid has been identified as a natural FXR antagonist, its elevated abundance observed in the present study may indicate potential modulation of FXR-related signalling, although FXR activity was not directly assessed. Similarly, previous studies have shown that excessive muricholic acid links to lipid metabolism disorders (Zheng et al. 2021), while elevated glycocholic acid correlates with hepatic fibrosis and cholangiocarcinoma (Proungvitaya et al. 2017; Yuan et al. 2023).

Ageing also led to increased xanthosine levels, likely reflecting elevated oxidative stress and inflammatory activity (Kudryavtseva et al. 2016). Xanthosine is involved in purine metabolism and serves as a precursor to guanosine (Furuhashi 2020). In skeletal muscle, xanthosine is involved in the purine nucleotide cycle, which contributes to ATP regeneration during periods of high energy demand (Ipata & Pesi 2018). Elevated xanthosine may therefore indicate increased nucleotide turnover, metabolic stress, and mitochondrial dysfunction, as observed during muscle ageing. Additionally, previous studies have linked higher xanthosine levels to inflammation and neurodegenerative conditions such as Alzheimer's disease, consistent with its association with systemic oxidative stress in the current study (Ansoleaga et al. 2015; Prestwich et al. 2013). These findings suggest that xanthosine may serve as a metabolic marker of both muscle energy dysregulation and age-related inflammatory stress.

Ginger supplementation induced selective changes in metabolite expression, suggesting potential antioxidant, anti-inflammatory, and muscle-preserving effects. In ginger-treated old rats, β-muricholic acid and xanthosine levels decreased, while γ-L-glutamyl-L-glutamic acid and 2,5-dimethylpyrazine increased (Table 2). Although tissue pharmacokinetics were not evaluated in the present study, previous animal studies have shown that orally administered 6-gingerol and 6-shogaol are rapidly absorbed into the systemic circulation and distributed to peripheral tissues (Jiang, Wang & Mi 2008; Li et al. 2019; Songvut et al. 2024). Following absorption, these compounds undergo extensive phase II metabolism and are predominantly present as glucuronide and sulfate conjugates (Li et al. 2019; Songvut et al. 2024). Although their distribution to skeletal muscle has not been directly quantified, their widespread tissue distribution supports the possibility that ginger-derived compounds or their metabolites reach skeletal muscle. This may explain the metabolomic changes observed following ginger supplementation.

In aged rats, ginger treatment reduced β-muricholic acid levels, suggesting that ginger may modulate bile acid metabolism. As β-muricholic acid acts as a natural FXR antagonist (Gaillard et al. 2021), its reduction may indicate potential modulation of FXR signalling. Although previous studies have linked FXR signalling to lipid and glucose metabolism, the present study did not directly assess FXR activity or downstream molecular pathways. Therefore, the observed changes in β-muricholic acid should be interpreted as indirect evidence of a potential mechanism by which ginger exerts metabolic benefits in ageing tissues.

Similarly, xanthosine and uric acid were downregulated in ginger-treated old rats, suggesting that ginger may influence purine metabolism. Previous studies have reported that ginger has xanthine oxidase inhibitory effects, which have been associated with reduced oxidative stress (Mohd Sahardi et al. 2023; Nile & Park 2015). Xanthine oxidase catalyses the conversion of hypoxanthine to xanthine and xanthine to uric acid (Packer 2020); the observed reductions in xanthosine and uric acid may reflect modulation of this metabolic pathway. However, xanthine oxidase activity was not directly measured in the present study. These findings also align with our previous study, which reported decreased uric acid levels in senescent myoblasts following ginger treatment (Mohd Sahardi et al. 2023). Although lower uric acid levels have been associated with reduced handgrip strength in older adults (Lee et al. 2019), the relationship between uric acid and skeletal muscle health remains complex and may be influenced by age-related changes in muscle composition, with fast-twitch fibres being more susceptible to oxidative stress than slow-twitch fibres (Drey 2011). These findings suggest that alteration in uric acid metabolism may reflect changes in oxidative status during ageing, although further studies are needed to establish the underlying mechanisms.

In addition, ginger supplementation was associated with increased levels of metabolites involved in glutathione (GSH) metabolism, including γ-L-glutamyl-L-glutamic acid in ginger-treated old rats. This metabolite is a product of glutamine degradation (Sebih et al. 2021). It serves as an indicator of GSH cycle function,

TABLE 2. List of significantly different metabolites in muscle of rats treated with ginger extract

Mode	Name	MW	RT	ID	FC			Overall p-value	FDR	Significant Tukey HSD comparisons
					YG vs YC	AG vs AC	OG vs OC			
pos	γ-L-Glutamyl-L-glutamic acid	276.09541	0.602	HMDB11737	-	-	+2.542	6.14×10^{-5}	6.29×10^{-4}	OG vs OC
pos	Uric acid	168.02825	1	HMDB00289	-	-	-3.473	2.77×10^{-4}	1.83×10^{-3}	OG vs OC
pos	Isomer: 2,5-Dimethylpyrazine/2,6-Dimethylpyrazine	108.06883	0.484	HMDB35289/HMDB35248	-	-	+1.421	8.38×10^{-4}	3.19×10^{-3}	OG vs OC
pos	2-Amino-4-methylpyrimidine	109.06414	0.483	MZ 3275	-	+1.270	-	8.69×10^{-3}	1.76×10^{-2}	AG vs AC
neg	Pantothenic acid	219.11009	3.51	HMDB00210	+1.599	-	-	1.20×10^{-6}	2.98×10^{-5}	YG vs YC
neg	β-Muricholic acid/Cholic acid	408.28746	9.861	HMDB0000415/HMDB00619	-	-	-5.211	2.43×10^{-4}	1.72×10^{-3}	OG vs OC
neg	Azelaic acid	188.10407	6.326	HMDB00784	-1.718	-	-	5.11×10^{-3}	1.25×10^{-2}	YG vs YC
neg	Xanthosine	284.07543	3.092	HMDB00299	-	-	-2.281	9.12×10^{-3}	1.80×10^{-2}	OG vs OC

MW: molecular weight; RT: retention time; FC, fold change; FDR, false discovery rate; YC, young control; AC, adult control; OC, old control; YG, young ginger-treated; AG, adult ginger-treated; OG, old ginger-treated. Overall p-values were obtained using one-way ANOVA and adjusted for multiple testing using the false discovery rate (FDR) method. Metabolites with FDR < 0.05 were considered statistically significant. Significant pairwise differences were identified using Tukey's HSD post-hoc test. The reported FDR values represent the overall ANOVA FDR and not individual Tukey pairwise FDR values

which contributes to the cell's antioxidant defences in response to oxidative stress (Sebih et al. 2021). Previous studies have shown that both glutamine availability and γ-L-glutamyl-L-glutamic acid regenerative capacity decline with ageing (Shang et al. 2020). Therefore, the upregulation of this metabolite following ginger treatment may suggest enhanced glutamine metabolism and antioxidant capacity. As glutamine metabolism has been linked to satellite cell proliferation, differentiation and mTOR signalling in previous studies (Sebih et al. 2021; Shang et al. 2020), the present findings may indicate a potential association between ginger supplementation and pathways involved in muscle regeneration. However, satellite cell activity, mTOR signalling, and GSH enzyme activities were not directly evaluated in this study.

Correlation analysis further reinforced these mechanistic insights. Several metabolites, including γ-L-glutamyl-L-glutamic acid, malic acid and coumarin, showed strong positive correlations with lipid peroxidation (r=0.48-0.58) (Supplementary Figure 1-data not shown), suggesting their sensitivity to oxidative stress. In contrast, amino acid-related metabolites such as thiamine, leucine/isoleucine, β-leucine, and phenylalanine showed moderate to strong negative correlations with the antioxidant enzymes catalase and SOD (r = -0.50 to -0.60), indicating improved redox balance in ginger-treated rats. Additionally, uric acid and xanthosine were positively associated with isoprostane levels, further supporting their role as markers of oxidative stress, while pantothenic acid and taurine showed significant negative correlations.

Beyond these ginger-mediated antioxidant and regenerative effects, pathway-level analysis further elucidates the broader metabolic alterations associated with ageing. Pathway analysis further substantiated these findings, identifying the phenylalanine, tyrosine, and tryptophan biosynthesis pathway and phenylalanine metabolism as significantly impacted ($p < 0.05$; impact > 0.1) (Figure 3 & Table 3), highlighting the central role of amino acid metabolism in ageing-associated muscle dysfunction. However, no significant and impactful pathways were identified in the ginger-treated group (Figure 4 & Table 4). Consistent with these alterations in amino acid-related pathways, amino acids essential for muscle maintenance, including leucine, lysine, and pipecolic acid, were upregulated in older rats, potentially reflecting a compensatory mechanism to

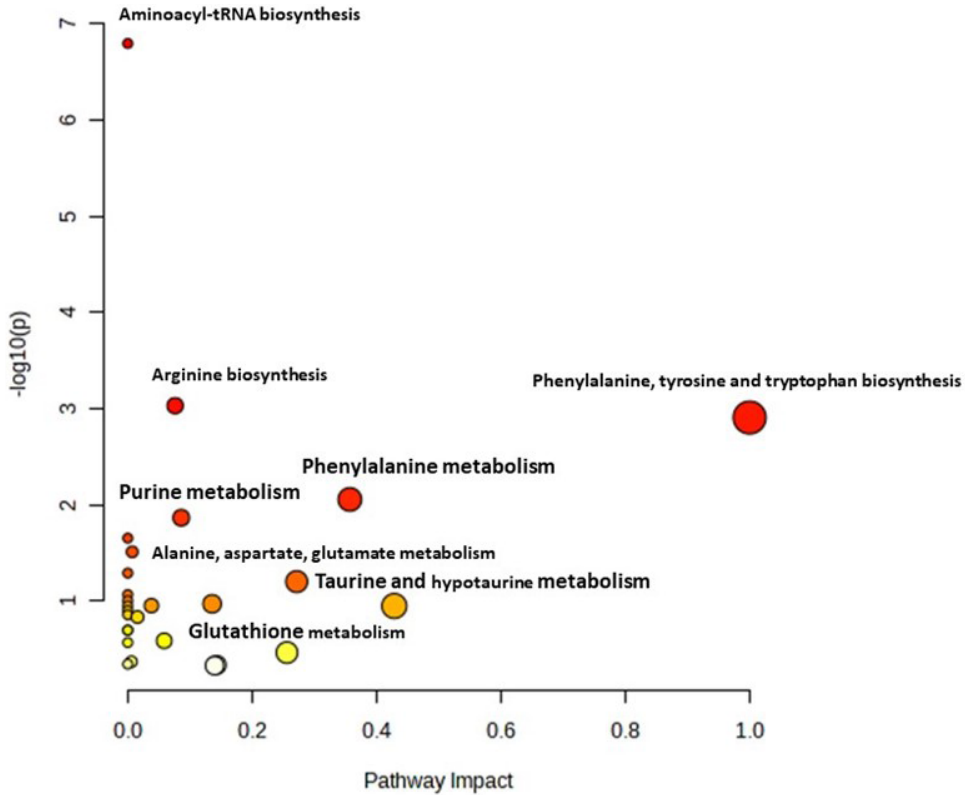


FIGURE 3. Biochemical pathway analysis of significantly different metabolites in control groups (young, adult, and old rats). The pathway analysis was performed using significantly altered metabolites identified by untargeted LC-MS/MS metabolomics analysis. The x-axis represents the pathway impact, while the y-axis represents pathway enrichment significance. Bubble size indicates pathway impact, and bubble colour represents the level of statistical significance

TABLE 3. List of biochemical pathways associated with significantly different metabolites in control groups (young, adult and old rats)

Pathway name	p-value	Impact
Aminoacyl-tRNA biosynthesis	1.6057E-7	0.0
Arginine biosynthesis	9.3498E-4	0.07614
Phenylalanine, tyrosine and tryptophan biosynthesis*	0.0012417	1.0
Phenylalanine metabolism*	0.0088204	0.35714
Purine metabolism	0.013673	0.08596
Histidine metabolism	0.022282	0.0
Pantothenate and CoA biosynthesis	0.030907	0.00714
Lysine degradation	0.051384	0.0
Primary bile acid biosynthesis	0.14716	0.01563
Butanoate metabolism	0.2017	0.0
Nicotinate and nicotinamide metabolism	0.2017	0.0

*Considered as significant biochemical pathway with p value <0.05 and impact value > 0.1

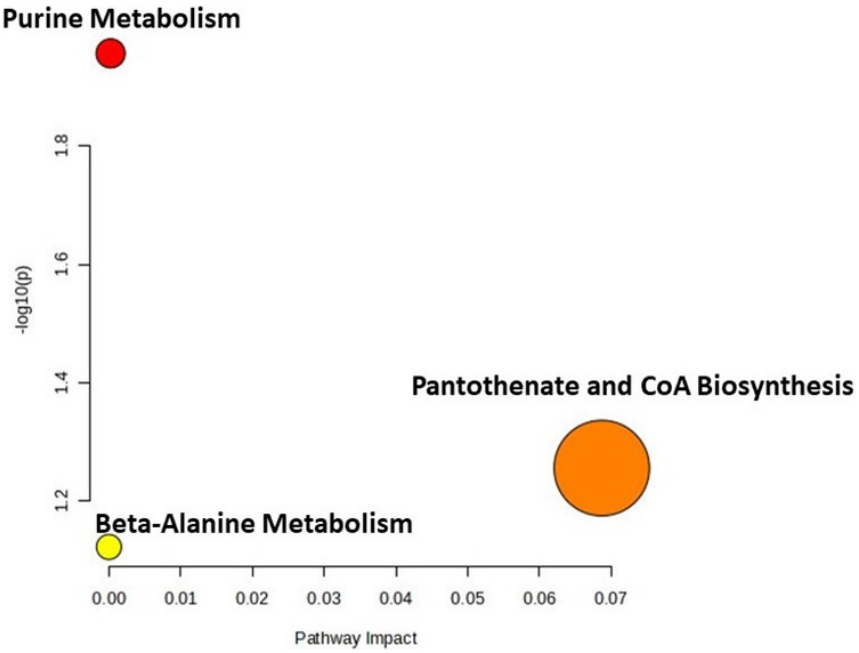


FIGURE 4. Biochemical pathway analysis of significant metabolites profiled for the ginger-treated group (young, adult and old rats). The pathway analysis was performed using significantly altered metabolites identified by untargeted LC-MS/MS metabolomics analysis. The x-axis represents the pathway impact, while the y-axis represents pathway enrichment significance. Bubble size indicates pathway impact, and bubble colour represents the level of statistical significance

TABLE 4. List of biochemical pathways of significant metabolites profiled for the ginger-treated group (young, adult, and old rats)

Pathway name	p-value	Impact
Purine metabolism	0.011056	2.3849E-4
Pantothenate and CoA biosynthesis	0.055488	0.068702
Beta-Alanine metabolism	0.075402	0.0

sustain muscle protein synthesis, activate satellite cells, and preserve muscle mass via mTOR signalling (Duan et al. 2017; Jin et al. 2020; Sato, Ito & Nagasawa 2016).

Leucine, a branched-chain amino acid, stimulates muscle protein synthesis by activating mTORC1 and initiating mRNA translation, and its administration in aged muscle has been shown to inhibit atrophy by promoting satellite cell growth and collagen remodelling (Chae, Park & Park 2021; Petrocelli et al. 2021; Yoshizawa, Mochizuki & Sugahara 2013). Meanwhile, lysine contributes to energy production, cellular signalling, and carbohydrate metabolism and supports muscle growth by activating satellite cells through the mTOR pathway; it also enhances cell viability, protein synthesis, autophagy, and apoptosis regulation (Aggarwal & Bains 2022; Jin et al. 2020; Liu et al. 2022). Pipecolic acid, a lysine intermediate in the α-aminoadipic acid pathway, stimulates protein synthesis and reduces muscle protein degradation (Sato, Ito & Nagasawa 2016; Struys & Jakobs 2010) and has been positively associated with muscle mass and strength in humans (Zhao et al. 2018), despite declining with age. The observed elevations may result from several factors: a compensatory increase to maintain muscle mass, reduced utilisation or altered catabolism of these amino acids, and a response to oxidative stress and low-grade inflammation in ageing muscle. These adaptations likely help preserve muscle function, counteract sarcopenic progression, and maintain metabolic homeostasis despite age-associated declines in protein synthesis efficiency.

Consistent with the pathway-level findings, specifically the significant impact on the phenylalanine, tyrosine, and tryptophan biosynthesis pathway, elevated tryptophan levels in older rats further reflect disruption within this metabolic network. Tryptophan is an essential nutrient required for niacin (vitamin B3) synthesis, which supports DNA synthesis and energy metabolism (Cleminson et al. 2020). Under normal conditions, peripheral tryptophan is primarily metabolised in the liver via the kynurenine pathway by tryptophan 2,3-dioxygenase (TDO) (Ramprasath et al. 2021). However, during inflammation, pro-inflammatory cytokines such as IFN-γ activates indoleamine-2,3-dioxygenase (IDO), which converts tryptophan into kynurenine. Elevated kynurenine levels have been associated with decreased muscle size and strength as well as increased mitochondrial lipid peroxidation (Kaiser et al. 2019). Therefore, the higher tryptophan observed in aged rats may indicate impaired tryptophan metabolism, likely associated with increased oxidative stress and inflammation, as supported by its negative correlation with catalase in this study. Figure 5 summarises the significant metabolic changes in the control group. Meanwhile, Figure 6 summarises the significant metabolic changes between the control and ginger-treated groups.

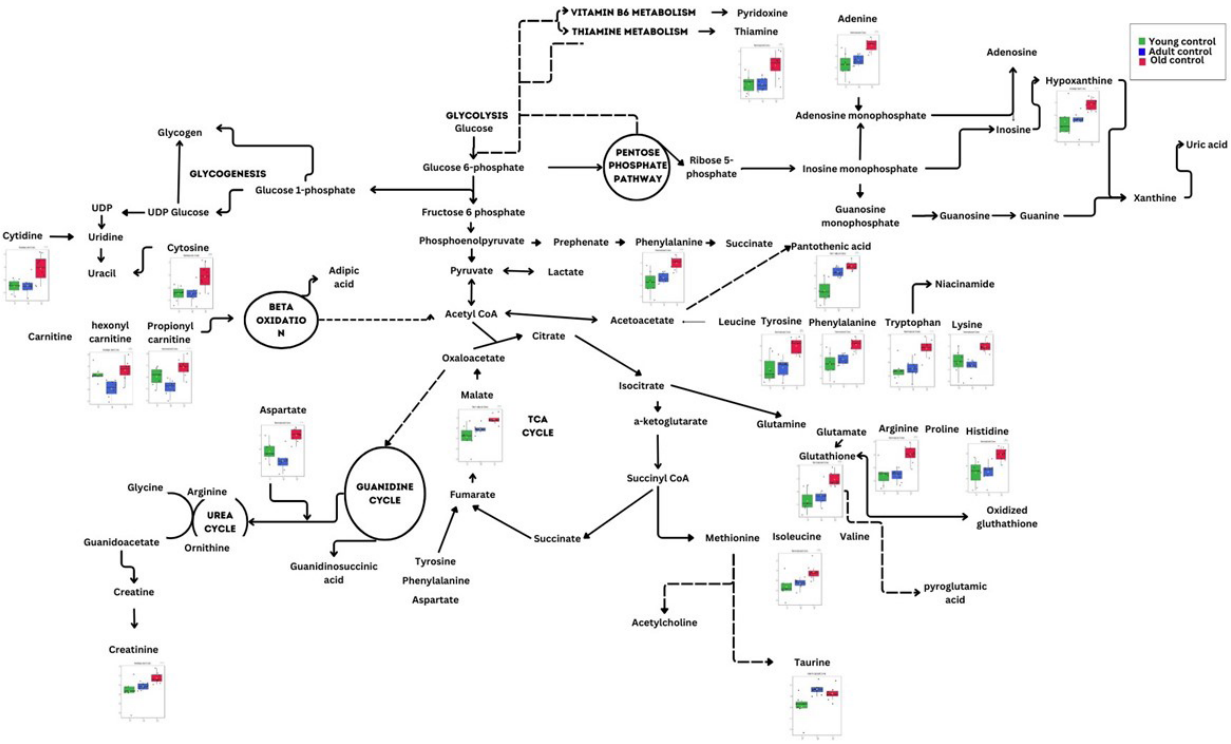


FIGURE 5. Summary of the significant metabolic changes in the control group

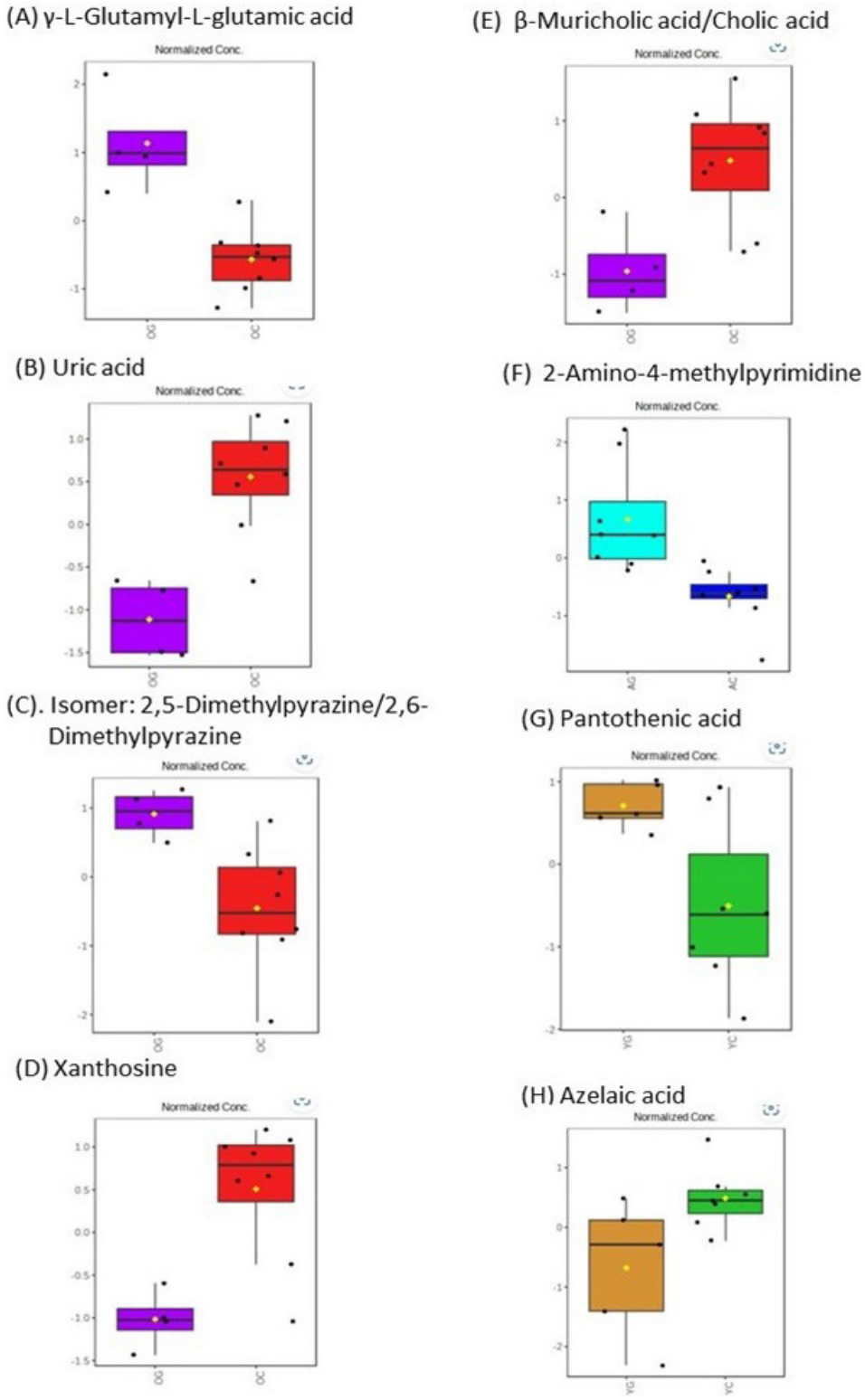


FIGURE 6. Significant metabolomic changes associated with age and ginger treatment. (A) γ-L-glutamyl-L-glutamic acid; (B) uric acid; (C) 2,5-dimethylpyrazine/2,6-dimethylpyrazine; (D) xanthosine; (E) β-muricholic acid/cholic acid; (F) 2-amino-4-methylpyrimidine; (G) pantothenic acid; and (H) azelaic acid. Metabolite concentrations in skeletal muscle specimens are shown graphically and compared. Box-and-whisker plots showing the median and interquartile range (IQR), with individual data points, are presented for each metabolite. Panels A–E compare old ginger-treated (OG) with old control (OC) rats, panel F compares adult ginger-treated (AG) with adult control (AC) rats, and panels G–H compare young ginger-treated (YG) with young control (YC) rats. Statistical significance was determined based on an FDR-adjusted p-value < 0.05

LIMITATIONS

Several limitations should be considered when interpreting these findings. Although metabolomics offers broad biochemical coverage, integrating proteomic, transcriptomic, or microbiome data would provide a more comprehensive understanding of pathway regulation during ageing. In addition, the number of metabolites significantly altered by ginger extract supplementation was relatively small and lacked a consistent age-dependent trend. This selective metabolic response may reflect the complex pharmacokinetics of ginger bioactive compounds, which undergo extensive metabolism and biotransformation after oral administration, as well as skeletal muscle's ability to maintain metabolic homeostasis. Consequently, ginger extract may primarily modulate specific metabolic pathways related to oxidative stress and energy metabolism rather than inducing widespread changes across the muscle metabolome. Nevertheless, the limited number of significantly altered metabolites reduced the ability to identify coordinated pathway-level changes in ginger-treated animals. Finally, a priori statistical power analysis was not performed, as the initial sample size was determined based on precedent from a previous animal study. Furthermore, although 10 animals were initially allocated to each group, two animals from the control group were excluded from the final analysis, resulting in unequal final sample sizes (control, n=8; ginger-treated, n=10). These factors may have reduced statistical power for detecting subtle metabolic differences and may contribute to the variability observed across age groups and treatment conditions.

CONCLUSIONS

In conclusion, ageing is associated with distinct metabolic alterations characterised by increased oxidative stress, inflammation, and impaired energy metabolism. Ginger supplementation partially mitigates these changes, supporting its potential role in enhancing antioxidant defences and promoting metabolic balance in ageing skeletal muscle.

ACKNOWLEDGEMENTS

This study was funded by the Dana Impak Perdana grant DIP-2024-016 from Universiti Kebangsaan Malaysia. The datasets generated and/or analysed during the current study are available from the corresponding author upon reasonable request.

REFERENCES

Abdul Sani, N.F., Belani, L.K., Pui Sin, C., Abdul Rahman, S.N.A., Das, S., Zar Chi, T., Makpol, S. & Yusof, Y.A.M. 2014. Effect of the combination of gelam honey and ginger on oxidative stress and metabolic profile in streptozotocin-induced diabetic Sprague-Dawley rats. *BioMed Research International* 2014: 160695.

Aggarwal, R. & Bains, K. 2022. Protein, lysine and vitamin D: Critical role in muscle and bone health. *Critical Reviews in Food Science and Nutrition* 62(9): 2548-2559.

Ansoleaga, B., Jové, M., Schlüter, A., Garcia-Esparcia, P., Moreno, J., Pujol, A., Pamplona, R., Portero-Otín, M. & Ferrer, I. 2015. Deregulation of purine metabolism in Alzheimer's disease. *Neurobiology of Aging* 36(1): 68-80.

Cannataro, R., Carbone, L., Petro, J.L., Cione, E., Vargas, S., Angulo, H., Forero, D.A., Odriozola-Martínez, A., Kreider, R.B. & Bonilla, D.A. 2021. Sarcopenia: Etiology, nutritional approaches, and miRNAs'. *International Journal of Molecular Sciences* 22(18): 9724.

Chae, M., Park, H.S. & Park, K. 2021. Association between dietary branched-chain amino acid intake and skeletal muscle mass index among Korean adults: Interaction with obesity. *Nutrition Research and Practice* 15(2): 203-212.

Cleminson, J.R., Stuart, A.L., Pasco, J.A., Hodge, J.M., Berk, M., Samarasinghe, R.M. & Williams, L.J. 2020. Dietary tryptophan and bone health: A cross-sectional, population-based study. *Archives of Osteoporosis* 15: 167.

Cruz-Jentoft, A.J. & Sayer, A.A. 2019. Sarcopenia. *Lancet* 393(10191): 2636-2646.

Cruz-Jentoft, A.J., Bahat, G., Bauer, J., Boirie, Y., Bruyère, O., Cederholm, T., Cooper, C., Landi, F., Rolland, Y., Sayer, A.A., Schneider, S.M., Sieber, C.C., Topinkova, E., Vandewoude, M., Visser, M. & Zamboni, M. 2019. Sarcopenia: Revised European consensus on definition and diagnosis. *Age and Aging* 48(1): 16-31.

Danial Efendy Goon, Sharaniza Ab-Rahim, Amir Hakimi Mohd Sakri, Musalmah Mazlan, Tan, Jen Kit, Mardiana Abdul Aziz, Mohd Noor Norizal, Effendi Ibrahim & Siti Hamimah Sheikh Abdul Kadir. 2021. Untargeted serum metabolites profiling in high-fat diet mice supplemented with enhanced palm tocotrienol-rich fraction using UHPLC-MS. *Scientific Reports* 11(1): 21001.

Dao, T., Green, A.E., Kim, Y.A., Bae, S.J., Ha, K.T., Gariani, K., Lee, M.R., Menzies, K.J. & Ryu, D. 2020. Sarcopenia and muscle aging: A brief overview. *Endocrinology and Metabolism* 35(4): 716-732.

Drey, M. 2011. Sarcopenia - Pathophysiology and clinical relevance. *Wiener Medizinische Wochenschrift* 161(17): 402-408.

Duan, Y., Zeng, L., Li, F., Wang, W., Li, Y., Guo, Q., Ji, Y., Tan, B.E. & Yin, Y. 2017. Effect of branched-chain amino acid ratio on the proliferation, differentiation, and expression levels of key regulators involved in protein metabolism of myocytes. *Nutrition* 36(1): 8-16.

Dunn, W.B., Broadhurst, D., Begley, P., Zelena, E., Francis-Mcintyre, S., Anderson, N., Brown, M., Knowles, J.D., Halsall, A., Haselden, J.N., Nicholls, A.W., Wilson, I.D., Kell, D.B. & Goodacre, R. 2011. Procedures for large-scale metabolic profiling of serum and plasma using gas chromatography and liquid chromatography coupled to mass spectrometry. *Nature Protocols* 6(7): 1060-1083.

Elhassan, Y.S., Kluckova, K., Fletcher, R.S., Schmidt, M.S., Garten, A., Doig, C.L., Cartwright, D.M., Oakey, L., Burley, C.V., Jenkinson, N., Wilson, M., Lucas, S.J.E., Akerman, I., Seabright, A., Lai, Y.C., Tennant, D.A., Nightingale, P., Wallis, G.A., Manolopoulos, K.N., Brenner, C., Philp, A. & Lavery, G.G. 2019. Nicotinamide riboside augments the aged human skeletal muscle NAD^+ metabolome and induces transcriptomic and anti-inflammatory signatures. *Cell Reports* 28(7): 1717-1728.e6.

Fleishman, J.S. & Kumar, S. 2024. Bile acid metabolism and signaling in health and disease: Molecular mechanisms and therapeutic targets. *Signal Transduction and Targeted Therapy* 9(1): 97.

Furuhashi, M. 2020. New insights into purine metabolism in metabolic diseases: Role of xanthine oxidoreductase activity. *American Journal of Physiology-Endocrinology and Metabolism* 319(5): E827-E834.

Gaillard, D., Masson, D., Garo, E., Souidi, M., Pais De Barros, J.P., Schoonjans, K., Grober, J., Besnard, P. & Thomas, C. 2021. Muricholic acids promote resistance to hypercholesterolemia in cholesterol-fed mice. *International Journal of Molecular Sciences* 22(13): 7163.

Guo, A., Li, K. & Xiao, Q. 2020. Fibroblast growth factor 19 alleviates palmitic acid-induced mitochondrial dysfunction and oxidative stress via the AMPK/PGC-1α pathway in skeletal muscle. *Biochemical and Biophysical Research Communications* 526(4): 1069-1076.

Ipata, P.L. & Pesi, R. 2018. Metabolic interaction between purine nucleotide cycle and oxypurine cycle during skeletal muscle contraction of different intensities: A biochemical reappraisal. *Metabolomics* 14(4): 42.

Jia, F., Liu, X. & Liu, Y. 2025. Bile acid signaling in skeletal muscle homeostasis: From molecular mechanisms to clinical applications. *Frontiers in Endocrinology (Lausanne)* 16(1): 1551100.

Jiang, S.Z., Wang, N.S. & Mi, S.Q. 2008. Plasma pharmacokinetics and tissue distribution of [6]-gingerol in rats. *Biopharmaceutics & Drug Disposition* 29(9): 529-537.

Jin, C.L., Zhang, Z.M., Song, Z.W., Gao, C.Q., Yan, H.C. & Wang, X.Q. 2020. mTORC1-mediated satellite cell differentiation is required for lysine-induced skeletal muscle growth. *Journal of Agricultural and Food Chemistry* 68(17): 4884-4892.

Kaiser, H., Yu, K., Pandya, C., Mendhe, B., Isales, C.M., McGee-Lawrence, M.E., Johnson, M., Fulzele, S. & Hamrick, M.W. 2019. Kynurenine, a tryptophan metabolite that increases with age, induces muscle atrophy and lipid peroxidation. *Oxidative Medicine and Cellular Longevity* 2019(1): 9894238.

Keitel, V., Stindt, J. & Häussinger, D. 2019. Bile acid-activated receptors: GPBAR1 (TGR5) and other G protein-coupled receptors. In Bile Acids and Their Receptors. Handbook of Experimental Pharmacology, vol. 256, edited by Fiorucci, S. & Distrutti, E. Cham: Springer. pp. 19-49.

Kudryavtseva, A.V., Krasnov, G.S., Dmitriev, A.A., Alekseev, B.Y., Kardymon, O.L., Sadritdinova, A.F., Fedorova, M.S., Pokrovsky, A.V., Melnikova, N.V., Kaprin, A.D., Moskalev, A.A. & Snezhkina, A.V. 2016. Mitochondrial dysfunction and oxidative stress in aging and cancer. *Oncotarget* 7(29): 44879-44905.

Lee, J., Hong, Y.S., Park, S.H. & Kang, K.Y. 2019. High serum uric acid level is associated with greater handgrip strength in the aged population. *Arthritis Research & Therapy* 21: 73.

Li, L.L., Cui, Y., Guo, X.H., Ma, K., Tian, P., Feng, J. & Wang, J.M. 2019. Pharmacokinetics and tissue distribution of gingerols and shogaols from ginger (*Zingiber officinale* Rosc.) in rats by UPLC-Q-Exactive-HRMS. *Molecules* 24(3): 512.

Liguori, I., Russo, G., Curcio, F., Bulli, G., Aran, L., Della-Morte, D., Gargiulo, G., Testa, G., Cacciatore, F., Bonaduce, D. & Abete, P. 2018. Oxidative stress, aging, and diseases. *Clinical Interventions in Aging* 13(1): 757-772.

Liu, M., Yue, Z., Zhang, B., Li, F., Liu, L. & Li, F. 2022. mTORC1 mediates the processes of lysine regulating satellite cells proliferation, apoptosis, and autophagy. *Metabolites* 12(9): 788.

Makpol, S., Abdul Sani, N.F., Hakimi, N.H., Ab Rani, N., Zakaria, S.N.A., Abd Rasid, A.F., Gunasekaran, G., Mohd Sahardi, N.F.N., Tan, J. K. & Abd Ghafar, N. 2020. *Zingiber officinale* Roscoe prevents DNA damage and improves muscle performance and bone integrity in old Sprague Dawley rats. *Evidence Based Complementary Alternative Medicine* 2020: 3823780.

Mohd Sahardi, N.F.N. & Makpol, S. 2019. Ginger (*Zingiber officinale* Roscoe) in the prevention of ageing and degenerative diseases: Review of current evidence. *Evidence Based Complementary Alternative Medicine* 2019: 5054395.

Mohd Sahardi, N.F.N., Jaafar, F., Tan, J.K., Mad Nordin, M.F. & Makpol, S. 2023. Elucidating the pharmacological properties of *Zingiber officinale* Roscoe (ginger) on muscle ageing by untargeted metabolomic profiling of human myoblasts. *Nutrients* 15(21): 4520.

Nile, S.H. & Park, S.W. 2015. Chromatographic analysis, antioxidant, anti-inflammatory, and xanthine oxidase inhibitory activities of ginger extracts and its reference compounds. *Industrial Crops and Products* 70(1): 238-244.

Packer, M. 2020. Uric acid is a biomarker of oxidative stress in the failing heart: Lessons learned from trials with allopurinol and SGLT2 inhibitors. *Journal of Cardiac Failure* 26(11): 977-984.

Petrocelli, J.J., Mahmassani, Z.S., Fix, D.K., Montgomery, J.A., Reidy, P.T., McKenzie, A.I., De Hart, N.M., Ferrara, P.J., Kelley, J.J., Eshima, H., Funai, K. & Drummond, M.J. 2021. Metformin and leucine increase satellite cells and collagen remodeling during disuse and recovery in aged muscle. *The FASEB Journal* 35(9): e21862.

Prestwich, E.G., Mangerich, A., Pang, B., Mcfaline, J.L., Lonkar, P., Sullivan, M.R., Trudel, L.J., Taghizedeh, K. & Dedon, P.C. 2013. Increased levels of inosine in a mouse model of inflammation. *Chemical Research in Toxicology* 26(4): 538-546.

Proungvitaya, S., Sombattheera, S., Boonsiri, P., Limpaiboon, T., Wongkham, S., Wongkham, C., Titapun, A. & Proungvitaya, T. 2017. Diagnostic value of serum bile acid composition patterns and serum glycocholic acid levels in cholangiocarcinoma. *Oncology Letters* 14(4): 4943-4948.

Ramprasath, T., Han, Y.M., Zhang, D., Yu, C.J. & Zou, M.H. 2021. Tryptophan catabolism and inflammation: A novel therapeutic target for aortic diseases. *Frontiers in Immunology* 12(1): 731701.

Razak, A.M., Zakaria, S.N.A., Abdul Sani, N.F., Ab Rani, N., Hakimi, N.H., Mohd Said, M., Tan, J.K., Gan, H.K., Mad Nordin, M.F. & Makpol, S. 2023. A subcritical water extract of soil grown *Zingiber officinale* Roscoe: Comparative analysis of antioxidant and anti-inflammatory effects and evaluation of bioactive metabolites. *Frontiers in Pharmacology* 14(1): 1006265.

Sahoo, B.M., Banik, B.K., Borah, P. & Jain, A. 2022. Reactive Oxygen Species (ROS): Key components in cancer therapies. *Anti-Cancer Agents in Medicinal Chemistry* 22(2): 215-222.

Sarip, M. 2012. Subcritical water extraction of 6-gingerol and 6-shogaol from *Zingiber officinale*. Thesis. Fakulti Kejuruteraan Kimia, Universiti Teknologi Malaysia.

Sato, T., Ito, Y. & Nagasawa, T. 2016. Regulatory effects of the L-lysine metabolites, L-2-aminoadipic acid and L-pipecolic acid, on protein turnover in C2C12 myotubes. *Bioscience Biotechnology and Biochemistry* 80(11): 2168-2175.

Saud Gany, S.L., Tan, J.K., Chin, K.Y., Hakimi, N.H., Ab Rani, N., Ihsan, N. & Makpol, S. 2022. Untargeted muscle tissue metabolites profiling in young, adult, and old rats supplemented with tocotrienol-rich fraction. *Frontiers in Molecular Biosciences* 9(1): 1008908.

Sebastiani, P., Monti, S., Lustgarten, M.S., Song, Z., Ellis, D., Tian, Q., Schwaiger-Haber, M., Stancliffe, E., Leshchyk, A., Short, M.I., Ardisson Korat, A.V., Gurinovich, A., Karagiannis, T., Li, M., Lords, H.J., Xiang, Q., Marron, M.M., Bae, H., Feitosa, M.F., Wojczynski, M.K., O'Connell, J.R., Montasser, M.E., Schupf, N., Arbeev, K., Yashin, A., Schork, N., Christensen, K., Andersen, S.L., Ferrucci, L., Rappaport, N., Perls, T.T. & Patti, G.J. 2024. Metabolite signatures of chronological age, aging, survival, and longevity. *Cell Reports* 43(11): 114913.

Sebih, F., Mokrane, N., Fontanel, P., Kayatekin, M., Kaabeche, M., Guiramand, J., Cohen-Solal, C., Cens, T., Rousset, M., Charnet, P., De Jésus Ferreira, M.C., Thibaud, J.B., Ménard, C., Cantel, S., Rolland, V., Vignes, M. & Roussel, J. 2021. The glutathione metabolite γ-glutamyl-glutamate partially activates glutamate NMDA receptors in central neurons with higher efficacy for GluN2B-containing receptors. *Frontiers in Pharmacology* 12(1): 794680.

Shang, M., Cappellesso, F., Amorim, R., Serneels, J., Virga, F., Eelen, G., Carobbio, S., Rincon, M.Y., Maechler, P., De Bock, K., Ho, P-C., Sandri, M., Ghesquière, B., Carmeliet, P., Di Matteo, M., Berardi, E. & Mazzone, M. 2020. Macrophage-derived glutamine boosts satellite cells and muscle regeneration. *Nature* 587(7835): 626-631.

Sies, H., Berndt, C. & Jones, D.P. 2017. Oxidative stress. *Annual Review of Biochemistry* 86(1): 715-748.

Songvut, P., Nakareangrit, W., Cholpraipimolrat, W., Kwangjai, J., Worasuttayangkurn, L., Watcharasit, P. & Satayavivad, J. 2024. Unraveling the interconversion pharmacokinetics and oral bioavailability of the major ginger constituents: [6]-gingerol, [6]-shogaol, and zingerone after single-dose administration in rats. *Frontiers in Pharmacology* 15: 1391019.

Struys, E.A. & Jakobs, C. 2010. Metabolism of lysine in α-aminoadipic semialdehyde dehydrogenase-deficient fibroblasts: Evidence for an alternative pathway of pipecolic acid formation. *FEBS Letters* 584(1): 181-186.

Tan, J.K., Zakaria, S.N.A., Gunasekaran, G., Abdul Sani, N.F., Nasaruddin, M.L., Jaafar, F., Abu Bakar, Z.H., Amir Hamzah, A.I.Z., Nor Aripin, K.N., Mohd Rani, M.D., Noh, N.A., Damanhuri, H.A., Mazlan, M., Makpol, S. & Wan Ngah, W.Z. 2023. Metabolomics profiling of age-associated metabolites in Malay population. *Oxidative Medicine and Cellular Longevity* 2023: 4416410.

Uchitomi, R., Hatazawa, Y., Senoo, N., Yoshioka, K., Fujita, M., Shimizu, T., Miura, S., Ono, Y. & Kamei, Y. 2019. Metabolomic analysis of skeletal muscle in aged mice. *Scientific Reports* 9(1): 10425.

Xia, J. & Wishart, D.S. 2016. Using MetaboAnalyst 3.0 for comprehensive metabolomics data analysis. *Current Protocols in Bioinformatics* 55(1): 14.10.11-14.10.91.

Yoshizawa, F., Mochizuki, S. & Sugahara, K. 2013. Differential dose response of mTOR signaling to oral administration of leucine in skeletal muscle and liver of rats. *Bioscience, Biotechnology, and Biochemistry* 77(4): 839-842.

Yuan, S. & Larsson, S.C. 2023. Epidemiology of sarcopenia: Prevalence, risk factors, and consequences. *Metabolism* 144(1): 155533.

Yuan, Z., Wang, J., Zhang, H., Chai, Y., Xu, Y., Miao, Y., Yuan, Z., Zhang, L., Jiang, Z. & Yu, Q. 2023. Glycocholic acid aggravates liver fibrosis by promoting the up-regulation of connective tissue growth factor in hepatocytes. *Cellular Signalling* 101(1): 110508.

Zhao, Q., Shen, H., Su, K-J., Tian, Q., Zhao, L-J., Qiu, C., Garrett, T.J., Liu, J., Kakhniashvili, D. & Deng, H-W. 2018. A joint analysis of metabolomic profiles associated with muscle mass and strength in Caucasian women. *Aging (Albany NY)* 10(10): 2624-2635.

Zheng, J., Ye, C., Hu, B., Yang, H., Yao, Q., Ma, J., Liu, Y. & Liu, H. 2021. Bile acid profiles in bile and feces of obese mice by a high-performance liquid chromatography-tandem mass spectrometry. *Biotechnology and Applied Biochemistry* 68(6): 1332-1341.